

Short communication

On the lithiation–delithiation of tin and tin-based intermetallic compounds on carbon paper current collector-substrate

C. Arbizzani, S. Beninati, M. Lazzari, M. Mastragostino*

Università di Bologna, Unità Complessa di Istituti di Scienze Chimiche, Radiochimiche e Metallurgiche, via San Donato 15, 40127 Bologna, Italy

Received 18 April 2005; received in revised form 3 June 2005; accepted 10 June 2005

Available online 7 November 2005

Abstract

With the aim to shed light on the effective role of carbon paper (CP) substrate-current collector on the constant capacity delivered over cycling by different types of anodes for lithium-ion batteries, $\text{Cu}_6\text{Sn}_5/\text{CP}$, $\text{Sn}_2\text{Mn}/\text{CP}$ and Sn/CP , we analyzed the voltage profiles of repeated galvanostatic charge/discharge cycles of these electrodes in terms of differential capacity (dQ/dV) versus voltage, comparatively with those of bare CP, and their structural modification by X-ray diffraction analysis before and after cycling. The results of this study demonstrate that Sn, in high mass loading electrodes, gradually loses the electric contact with the current collector and $\text{Sn}_2\text{Mn}/\text{CP}$ electrodes show a gradual degradation of Sn_2Mn . In both cases, CP is involved in the electrochemical process by contributing to the delivered capacity of these electrodes which display stability over 100 of cycles. Furthermore, the analysis of the $\text{Cu}_6\text{Sn}_5/\text{CP}$ electrodes, which for high mass loading were able to provide constant capacity significantly higher than that the bare CP supplied and to remain stable for a number of cycles higher than Sn and Sn_2Mn did, indicates that CP effect on the Cu_6Sn_5 cycling stability is moderate as it concerns the contribution to capacity but it is fundamental for the electric contact. Hence, CP can be considered an excellent substrate-current collector only for intermetallic compounds like Cu_6Sn_5 that contains an inert metal able to buffer the volume changes accompanying the lithiation processes which provide compounds isostructural with the unlithiated intermetallic up to 2.6Li/Sn atomic ratio ($\text{Li}_{13}\text{Cu}_6\text{Sn}_5$).

© 2005 Elsevier B.V. All rights reserved.

Keywords: Lithium-ion batteries; Anode materials; Lithiation/delithiation; Carbon paper

1. Introduction

Lithium/metal alloys would be suitable candidates to substitute graphite electrodes in lithium-ion batteries because of their high specific capacity, but the large volume changes due to the lithiation–delithiation processes, which are the main cause of the poor capacity retention upon cycling of these anode materials, are still their main drawback. Among the different approaches that have been pursued to overcome this trouble there was the yielding of nanomaterials and of intermetallic compounds, with the best results reached with nanostructured intermetallic compounds [1–3]. The small particle size of the electrode materials (metals or intermetallic compounds) improves significantly the electrode cycle life; the volume expansion due to the lithium insertion causes much less cracking and pulverization in nano-

sized metal alloys than in presence of coarse particles [4], and this is mostly true in the case of nanostructured intermetallic compounds, where there is also the contribution of the inactive metal which provides stability to the electrode material [5]. A more recent strategy is the use of nanocomposites based on lithium storage metals and carbonaceous materials, in which the conducting carbon hosts metal nanoparticles on its surface or into its porous structure. It has been reported that the uniform dispersion of a lithium storage material on the surface of a carbonaceous one, such as mesophase spherules or carbon nanotubes, improved the electrode cycleability because of the stabilization of the nanosized alloy particles against agglomeration during lithium insertion and deinsertion processes [6–8]. Metal/C composites were also obtained by infiltrating metal sources into polymers or carbonaceous materials followed by appropriate treatment, as in the case of Sn/polystyrene resin or Sn/activated carbon [9,10]. Given that metal alloys, intermetallic compounds or metal/C composites are generally mixed with a conductive agent and a binder before being laminated onto the

* Corresponding author. Tel.: +39 0512099798; fax: +39 0512099365.
E-mail address: marina.mastragostino@unibo.it (M. Mastragostino).

current collector, attention had been paid also to binder, which is of paramount importance to maintain cohesion between particles and current collector [4,11]. Given that also the choice of the current collector could be crucial, we focused our efforts on the study of anode materials, such as Cu_6Sn_5 and Sn on carbon paper current collectors rather than on copper foils or grids [12,13]. The particular choice of the CP, a commercial product constituted by a three-dimension network of conducting carbon fibers of 10 μm diameter, was done having in mind that CP was able to host among the fibers, the nanometric metal or intermetallic compound and to guarantee a better electric contact after a great number of charge/discharge cycles. We found, indeed, cycling stability over more than 100 cycles for $\text{Cu}_6\text{Sn}_5/\text{CP}$ electrodes, even with high electrode mass loading, and for Sn/CP less cycling stability than for $\text{Cu}_6\text{Sn}_5/\text{CP}$ although significantly better than that for Sn/Cu electrodes. In addition, we demonstrated that the bare CP, being a not totally amorphous carbonaceous material, was able to be lithiated–delithiated at more negative potentials than those of Sn and Cu_6Sn_5 , delivering constant capacity throughout at least 50 cycles, then sharply lost capacity.

With the aim to shed light on the effective role of carbon paper on cycling stability of tin and tin-based intermetallic hosted in CP substrate-current collector we prepared and tested the Sn_2Mn , and investigated the voltage profiles, compared to those of bare CP, of the three types of electrodes for lithium-ion batteries, $\text{Sn}_2\text{Mn}/\text{CP}$, $\text{Cu}_6\text{Sn}_5/\text{CP}$ and Sn/CP, during repeated galvanostatic cycles and their structural modifications by X-ray diffraction (XRD) analysis before and after cycling, and the results are here reported.

2. Experimental

The Sn_2Mn was electrodeposited by galvanostatic and potentiostatic techniques both on CP (Spectracorp. 2050, 10 mil, 10 mg cm^{-2}) and Cu current collectors from degassed, acid solutions (pH 2.5–3 with H_2SO_4) of 0.07 M SnSO_4 , 0.59 M MnSO_4 , 0.014 M sodium and potassium tartrate and 1 M $(\text{NH}_4)_2\text{SO}_4$, at room temperature after ref. [14]. Adhesive tape was used to prevent deposition on the back of the electrode and to limit the exposed area to 1 cm^2 . The galvanostatic deposition was carried out at -70 mA cm^{-2} (the mean voltage was ca. -1.7 V versus saturated calomel electrode, SCE); the potentiostatic deposition was performed only on Cu foil at -1.8 V versus SCE, whereas on CP pulsed potentiostatic deposition of Sn_2Mn was carried out in presence of higher concentration of MnSO_4 (0.90 M) with duty and rest time at -1.75 V versus SCE for 50 ms and -1.200 V for 300 ms, respectively, and a total duty time of 5880 s. The Sn_2Mn electrodes were dried under vacuum at 60°C for 16 h before use. Ultra pure water (MilliQ – 18.6 $\text{M}\Omega \text{ cm}$, Simplicity Water System, Millipore Co.) was employed for all the solutions and rinsing.

All the electrodes were characterized by X-ray diffraction analysis with a Philips PW1050/81 powder diffractometer ($\text{Cu K}\alpha$ radiation, 40 mA, 40 kV). Scanning electron microscopy (SEM) analyses were performed with a Philips 515 scanning electron microscope. All the electrodes were electrochemically characterized by galvanostatic charge/discharge cycles at

$T = 30 \pm 1^\circ\text{C}$ in a T-shaped cell sealed in dry-box (Mbraun Labmaster 130, O_2 and $\text{H}_2\text{O} < 1 \text{ ppm}$). The geometric area of the working electrode ranged from 0.68 to 0.71 cm^2 . The charge/discharge cycles were performed at 0.5 mA, so that the current density ranged from 0.74 to 0.70 mA cm^{-2} . The terms “charge” and “discharge” refer to lithiation and delithiation, respectively. The discharges were potential-limited and the charges were time-limited (while maintaining a safe voltage cut-off of 0.005 V versus Li) to insert defined amounts of lithium per atom of tin. The amount of the inserted lithium (estimated as product of current and time) was calculated, in relation to the Li/Sn atomic ratio to be reached, on the basis of the mass of the material loaded on the electrode. The counter electrode was metallic Li in excess and the reference electrode for monitoring the electrode potentials was a Li foil. The separator, a Whatman GF/D glass fiber disk, was imbibed with the electrolyte solution ethylene carbonate:dimethylcarbonate (EC:DMC 2:1)—1 M LiPF_6 (LP31 Merck, battery grade). The electrochemical deposition and characterization were performed with a Radiometer Voltmaster PGZ 301 potentiostat/galvanostat and a Perkin-Elmer VMP multichannel potentiostat, respectively.

3. Results and discussion

In a previous paper, we demonstrated that $\text{Cu}_6\text{Sn}_5/\text{CP}$ electrodes, differently from $\text{Cu}_6\text{Sn}_5/\text{Cu}$ electrodes, can stand more than hundred cycles at high current density and with Li/Sn atomic ratio ≥ 2 without capacity loss. In particular, electrodes with 7.5 mg cm^{-2} (weight of the non-lithiated compound) and charge limited to 2.08 Li/Sn atomic ratio showed specific capacity values of 280 mAh g^{-1} and geometric capacity of 2.1 mAh cm^{-2} over 150 cycles [12].

We also studied the performance of Sn/CP electrodes to verify if the use of CP instead of Cu could bring substantial improvements on the cycleability of Sn, just like in the case of $\text{Cu}_6\text{Sn}_5/\text{CP}$ electrodes. The Sn/CP electrodes, with charge limited up to 2.1 Li/Sn atomic ratio, showed cycling stability higher than that of Sn/Cu electrodes, however, lower than that of $\text{Cu}_6\text{Sn}_5/\text{CP}$ with comparable mass loading, demonstrating that the use of the intermetallic compound with an inert metal buffering the Sn volume variations is still the best strategy for having electrodes with high cycling stability [13].

To investigate if all the Sn-based intermetallic compounds behave in the same way, we prepared electrodes of Sn_2Mn electrochemically deposited both on CP and on Cu. The cycling behavior of Sn_2Mn on Cu had been already investigated by Beaulieu et al. [15] and they reported that Sn_2Mn capacity decreased to 0 after 20 cycles; improved results in cycling stability were obtained for Sn–Mn–C composites on Cu but with low charge delivered [16]. The choice of Sn_2Mn could be debatable because Sn_2Mn , in which the lithiation process produces Li_xSn with the extrusion of Mn, could be more liable to capacity loss over repeated lithiation/delithiation than Cu_6Sn_5 which shows structural compatibility with its lithiated form up to 2.6 Li/Sn ($\text{Li}_{13}\text{Cu}_6\text{Sn}_5$).

For the characterization of the electrodeposited Sn_2Mn , we performed XRD analysis that demonstrated that the deposits

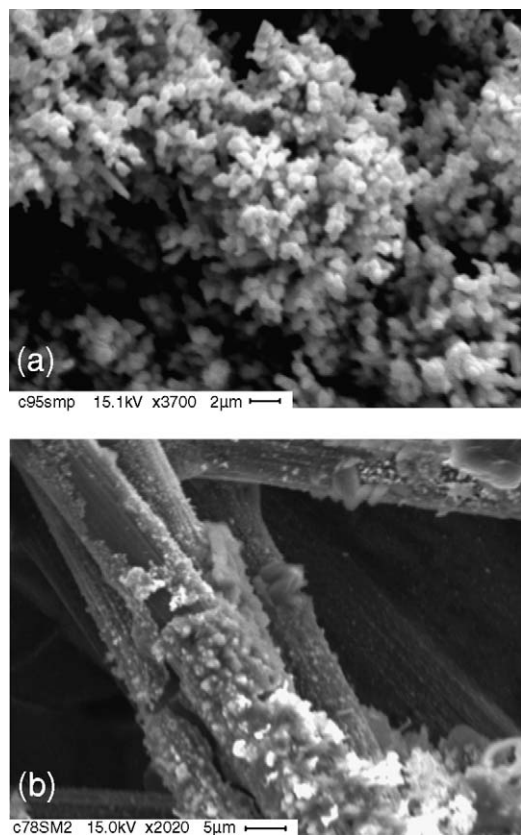


Fig. 1. SEM images at different magnification of Sn_2Mn yielded on CP (a) by pulsed potentiostatic deposition and (b) by galvanostatic deposition.

contained two crystalline phases, Sn and Sn_2Mn (see infra). The SEM image of Fig. 1 shows that for the material electrodeposited on CP, particularly in the case of pulsed potentiostatic deposition, the covering of carbon fibers was homogeneous, with submicrometric-sized aggregates constituted by 30 nm particles (estimated size from XRD analysis).

Electrodes with Sn_2Mn mass loading of 2–3 mg cm^{-2} were tested by repeated lithiation/delithiation galvanostatic cycles with charge process limited in time to insert a fixed lithium amount (2 Li/Sn atomic ratio, by considering that all the material deposited was Sn_2Mn) and with the 0.005 V safety cut-off voltage; the discharge process was limited to 1.3 V versus Li. With this intermetallic compound, like with Cu_6Sn_5 and Sn, a complete capacity loss after ca. 30 cycles was observed if Cu current collectors were used. By contrast, $\text{Sn}_2\text{Mn}/\text{CP}$ gave a constant capacity of ca. 0.9 mAh cm^{-2} , i.e. 350 mAh g^{-1} , over 100 cycles, as shown in Fig. 2. The low capacity value per geometric area is related to the low Sn_2Mn mass loading, given that the hydrogen evolution during the electrochemical deposition did not permit to yield heavier deposits. Fig. 2 also shows the geometric and specific capacity values over cycling of selected $\text{Cu}_6\text{Sn}_5/\text{CP}$ [12] and Sn/CP [13] electrodes for comparison.

With the purpose to clarify the effective role of CP on the cycling stability of the three kind of electrodes, we analyzed the voltage profiles during lithiation/delithiation cycles in terms of differential capacity (dQ/dV) versus voltage to clearly evidence the evolution of the lithiation/delithiation process and we

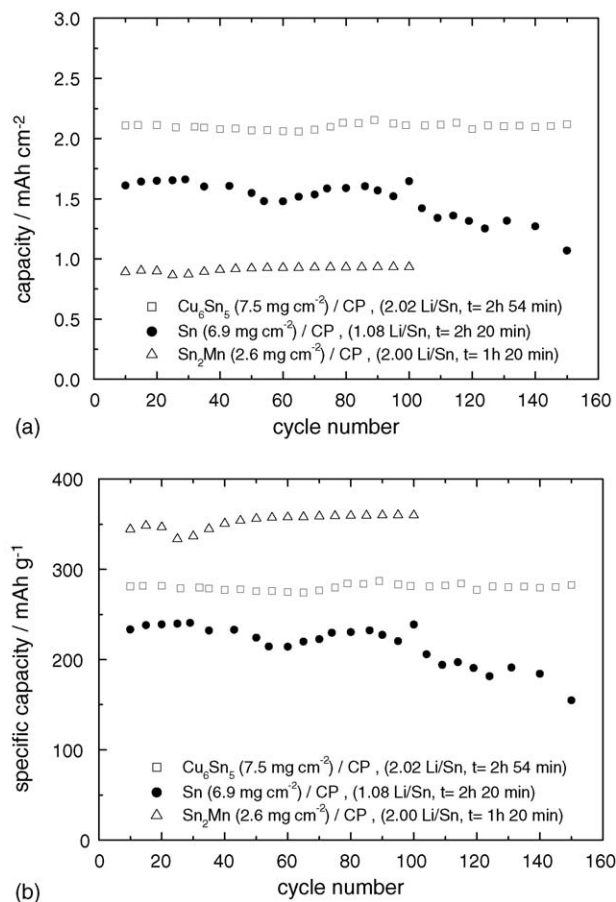


Fig. 2. Geometric capacity (a) and specific capacity (b) of $\text{Cu}_6\text{Sn}_5/\text{CP}$, Sn/CP and $\text{Sn}_2\text{Mn}/\text{CP}$ electrodes. In the figures, the masses of active material, the Li/Sn atomic ratios and the set charge times are indicated.

carried out the XRD analysis of the electrodes before and after cycling.

Fig. 3 displays the differential capacity at different cycle number of $\text{Cu}_6\text{Sn}_5/\text{CP}$, Sn/CP and $\text{Sn}_2\text{Mn}/\text{CP}$ electrodes and of the bare CP. The dQ/dV versus V plots of the lithium insertion are in Fig. 3a–d and those of lithium deinsertion are in Fig. 3a'–d'. In Figs. 3a–c and a'–c', are also reported for comparison the differential capacity plots of one selected charge/discharge cycle of bare CP to be compared with the last cycle of tin and intermetallic electrodes. In the case of high mass loading $\text{Cu}_6\text{Sn}_5/\text{CP}$ and Sn/CP electrodes, whose charge time was 2 h 54 min and 2 h 20 min, respectively, the CP selected for comparison was tested with charge not limited in time, but only limited in voltage. When the bare CP electrodes were tested by setting a limitless charge time they delivered a constant capacity of 1.4 mAh cm^{-2} , i.e. 140 mAh g^{-1} , during the first 50 cycles, then, the capacity decreased sharply; however, over more than 10 tested bare CP electrodes, we found one able to sustain more than 100 cycles with charge time of ca. 2 h, and this demonstrates the poor reproducibility of the lithiation–delithiation processes of CP. The dQ/dV versus V plots of the CP electrode tested by setting a limitless charge time in Fig. 3d and d' shows that the lithium insertion in CP begins well below 0.25 V, with the plateau centered at ca. 0.05 V, whereas the lithium deinsertion starts above

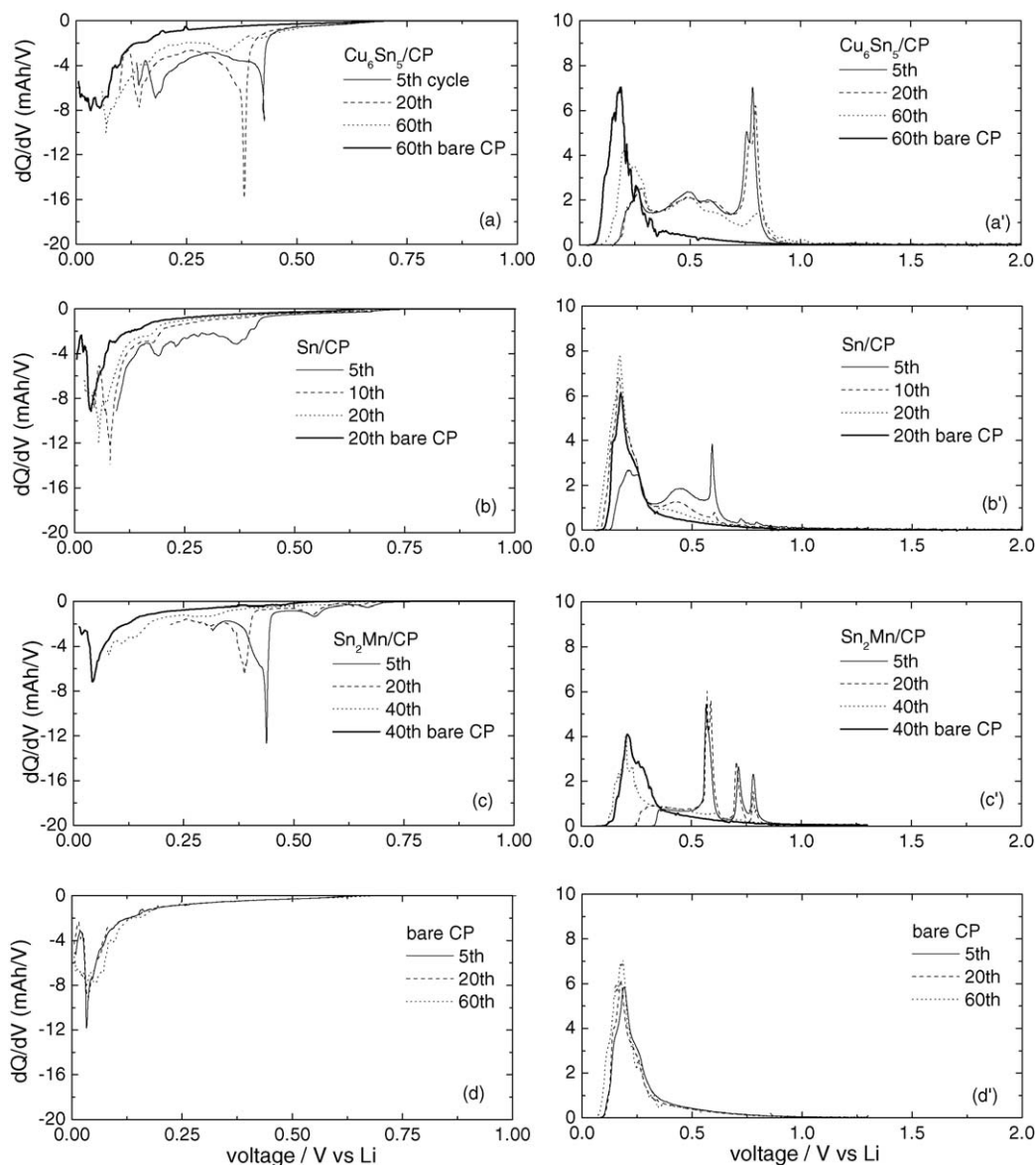


Fig. 3. dQ/dV vs. V plots of the (a–d) insertion and (a'–d') deinsertion processes of the $\text{Cu}_6\text{Sn}_5/\text{CP}$, Sn/CP and $\text{Sn}_2\text{Mn}/\text{CP}$ electrodes of Fig. 2 and of bare CP. (a and a') $\text{Cu}_6\text{Sn}_5/\text{CP}$, 7.5 mg cm^{-2} active material, 2.02 Li/Sn, charge time 2 h 54 min; (b and b') Sn/CP , 6.9 mg cm^{-2} active material, 1.08 Li/Sn, charge time 2 h 20 min; (c and c') $\text{Sn}_2\text{Mn}/\text{CP}$, 2.6 mg cm^{-2} active material, 2.00 Li/Sn, charge time 1 h 20 min; (d and d') bare CP, 6.8 mg cm^{-2} , the charge time was unlimited (however, charge process ended after ca. 2 h).

0.05 V, with the plateau centered at ca. 0.185 V, and at ca. 0.4 V, the delithiation process is almost complete.

The main difference in the patterns of $\text{Cu}_6\text{Sn}_5/\text{CP}$, Sn/CP and $\text{Sn}_2\text{Mn}/\text{CP}$ electrodes and of the bare CP is the shape of the peaks of the lithiation/delithiation, sharp those of the tin and tin-based intermetallics, broad those of the CP, due to the fact that CP is not crystalline, even if not completely amorphous, while tin or tin-based compounds are nanocrystalline. In addition the lithium insertion in intermetallic hosts begin at 0.5 V (tin alone begins to insert at 0.75 V) and lithium deinsertion takes place above 0.3 V and at ca. 0.9 V is complete. The differential analysis of voltage profiles of the $\text{Cu}_6\text{Sn}_5/\text{CP}$ electrode in Fig. 3a and a' shows that the characteristic peaks of the lithiation/delithiation plateau of this intermetallic are present for a number of cycles higher than those of Sn/CP and $\text{Sn}_2\text{Mn}/\text{CP}$ electrodes (Fig. 3b

and b' and c and c', respectively) and the characteristic peaks of CP (at potential lower than 0.25 V) gradually appear. The $\text{Cu}_6\text{Sn}_5/\text{CP}$ never reached the 0.005 V cut-off even if the potential at the end of the insertion process (charge time set to 2 h 54 min, Li/Sn = 2.02) gradually shifted toward less positive values (the 5th, 20th and 60th cycles considered in Fig. 3a and a' reached 0.14, 0.10 and 0.06 V, respectively); this is the reason of the increasing, over cycling, of the peak attributed to the delithiation of CP, which contributes to the total capacity of the electrode. However, the fact that the Cu_6Sn_5 electrodes with high intermetallic mass loading are able to provide constant capacity values significantly higher than those delivered by CP indicates that the contribution of CP to the maintenance of the capacity of Cu_6Sn_5 is moderate as regards the amount of charge involved in the lithiation process, but extremely important for the preserva-

tion of the electric contact. The decreasing of the peaks related to the intermetallic delithiation at the 60th cycle indicates that Cu_6Sn_5 modifies its properties, but it still remains able to sustain lithium insertion–delithiation cycles. In the case of tin, we found a different behavior. The decrease, in Fig. 3b and b', of the peaks attributable to the lithiation/delithiation processes of Sn and the rising of the characteristic CP peaks occur in very few cycles. Although the 5th, 10th and 20th cycles considered in Fig. 3b and b' reached 0.10, 0.04 and 0.02 V, respectively, at the end of charge (charge time set to 2 h 20 min, $\text{Li}/\text{Sn} = 1.08$) and the 0.005 V cut-off was reached after the 25th cycle, the contribution of CP to the lithiation/delithiation processes of the electrode seems more important; the total disappearance of the Li deinsertion peaks from Sn and the similarity of the two plots of Fig. 3b' related to the 20th cycle of Sn/CP and of bare CP indicates that the process of delithiation has to be ascribed almost totally to CP in this electrode of high mass loading. In the case of $\text{Sn}_2\text{Mn}/\text{CP}$ electrode (Fig. 3c and c'), due to a lower intermetallic mass loading, the time set for charge was lower (1 h 20 min, $\text{Li}/\text{Sn} = 2.00$) than that set for Cu_6Sn_5 and Sn. The decrease and disappearance of the peaks attributable to the lithiation/delithiation processes of Sn_2Mn and the rising of the characteristic CP peaks occurred in 40 cycles. As in the case of $\text{Cu}_6\text{Sn}_5/\text{CP}$, the $\text{Sn}_2\text{Mn}/\text{CP}$ electrode never reached the 0.005 V over 100 cycles, and attained the voltage of 0.31, 0.22 and 0.08 V, respectively, at the end of the 5th, 20th and 40th charge. Due to the potential values at the end of the charge, well above the lithium insertion potentials in CP, in the first 20–30 cycles the contribution of CP to the lithiation/delithiation processes of the electrode, in terms of capacity, is negligible, as the absence of the peak related to CP in Fig. 3c and c' gives evidence. However, the differential capacity plot of the $\text{Sn}_2\text{Mn}/\text{CP}$ electrode shows the evolution of the characteristic peaks of the lithiation–delithiation plateau of the intermetallic, to which corresponds an increase of the lithiation peaks of CP, up to their total disappearance between the 30th and 40th cycles. This explains the small minimum in capacity observed in correspondence of the 30th–40th cycle in all the $\text{Sn}_2\text{Mn}/\text{CP}$ samples which testifies not only the modification of the Sn_2Mn over cycling but also the exchange of the material which undergoes the lithiation/delithiation process, from Sn_2Mn to CP.

Fig. 4 shows the XRD patterns of $\text{Cu}_6\text{Sn}_5/\text{CP}$, Sn/CP and $\text{Sn}_2\text{Mn}/\text{CP}$ electrodes before and after cycling. In Fig. 4a, the characteristic reflections of Cu_6Sn_5 are still present after cycling showing a slight broadening which could indicate a moderate loss of crystallinity over cycling. This behavior is representative of a material that evolves during cycling without significant degradation, even if the presence of the reflections at 40.5° and 47.5° attributable to the lithiated Cu_6Sn_5 could indicate that some regions become electrically isolated.

In Fig. 4b, the reflections of Sn remain unchanged before and after cycling, demonstrating that Sn was still on the electrode and it was not deteriorated. Taking into account the disappearance of the peaks related to Sn in the plot of Fig. 3b', a gradual loss of contact of Sn with the current collector can explain the behavior of the Sn/CP electrode. Therefore, the CP, although more pliant than Cu, is unable to maintain the electric contact in high mass loading Sn/CP electrodes (presumably for parti-

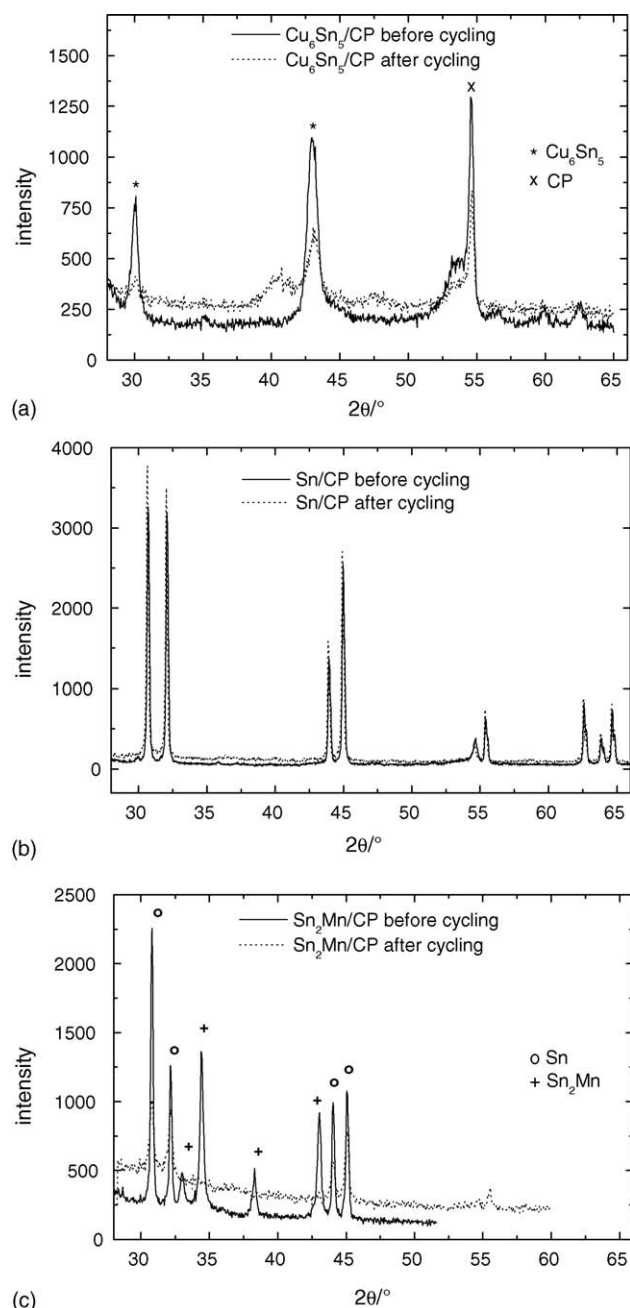


Fig. 4. Diffraction patterns of (a) $\text{Cu}_6\text{Sn}_5/\text{CP}$, (b) Sn/CP and (c) $\text{Sn}_2\text{Mn}/\text{CP}$ before cycling (solid line) and after 100 galvanostatic charge/discharge cycles (dotted line). The main diffraction peaks of CP (x), Cu_6Sn_5 (*) , Sn (o) and Sn_2Mn (+) are also indicated.

cles aggregation after the great Sn volume changes) and when the electric contact is lost it sustains the electrode cycling by contributing with its lithiation/delithiation capacity (maximum values of ca. 1.4 mAh cm^{-2}).

In Fig. 4c, the situation is completely different from that of Fig. 4a and b: after 100 cycles, there is the total loss of the characteristic reflections of Sn_2Mn and a strong reduction accompanied by a small enlargement of the diffraction peaks of the Sn phase initially present (in some samples it was observed the total disappearance of Sn reflections). Fig. 4c demonstrates that the Sn_2Mn intermetallic compound is destroyed over cycling, according

also with data in Fig. 3c and c' , and the constant capacity of ca. 0.9 mAh cm^{-2} delivered by these electrodes up to the 100th cycle is due to the fact that the capacity loss related to the destruction of the Sn_2Mn is compensated by the lithiation process of CP which is able to deliver this capacity for 100 cycles.

Hence, we have demonstrated that the role of CP as current collector-substrate in cycling stability of tin and tin-based intermetallic compounds is not negligible. When, in the case of Sn and Sn_2Mn , the material hosted in CP loses electroactivity, because of detachment or degradation, the CP substitutes it, completely or in part, in the lithiation/delithiation processes, thus contributing to the whole electrode's life and apparently improving the materials performance. By contrast, the good cycling performance of the $\text{Cu}_6\text{Sn}_5/\text{CP}$ electrodes is due to the CP three-dimension network which is able to preserve the electric contact with the particle agglomerates of Cu_6Sn_5 (even when there is formation of some cracks in the material due to the volume variations). Thus, CP is an excellent current collector-substrate for Cu_6Sn_5 , which takes advantage from structural stability up to lithium insertion of 2.6 Li/Sn atomic ratio, even because it makes unnecessary the addition of conductive carbon, differently from graphite in commercial lithium-ion batteries, a fact that makes the geometric and specific capacity values (2.1 mAh cm^{-2} , 280 mAh g^{-1}) of particular interest when compared to those of graphite composite electrodes. The comparison is more favorable when the mass of the current collectors, too, is taken into account, because the CP mass (10 mg cm^{-2}) is lower than that of Cu foil used for the negative electrode of commercial lithium batteries [17]. From the volumetric point of view, the CP we used was not the optimum choice; with thinner CP, which is also commercially available, it should be possible to reach volumetric specific capacity values of $200\text{--}300 \text{ mAh cm}^{-3}$, near to those of commercial batteries with graphite anodes on Cu foil ($18 \mu\text{m}$) having volumetric capacity from 230 to 450 mAh cm^{-3} and total anode thickness of ca. $185\text{--}200 \mu\text{m}$ [17].

4. Conclusions

On the basis of these results we can state that CP is an excellent current collector-substrate for a nanostructured intermetallic compound, such as Cu_6Sn_5 that, in addition to the buffering properties on volume variations of the inert metal, is able to insert lithium maintaining a good structural stability, due to the fact that the $\text{Li}_{13}\text{Cu}_6\text{Sn}_5$ is isostructural with Cu_6Sn_5 . This means that the morphology of CP assists in preserving the electric contact during the lithiation/delithiation processes when the volume expansions are not too much high. On the contrary, an intermetallic compound, such as Sn_2Mn , even if an inert metal is present, cannot take advantage from the ameliorated electric contact with CP because of its structural modification over repeated lithiation–delithiation processes. Also pure tin, whose lithiation

provokes great dimensional changes, cannot take enough advantage from the ameliorated electric contact with CP. However, given that CP itself can be reversibly lithiated, it contributes to maintain constant capacity for a high number of cycles even when there is a complete loss of contact with the anode material or when material degradation takes place, thus contributing to a longer cycle life of the electrode as a whole. It should be interesting to evaluate the influence of the CP substrate-current collector also on cathode materials; in this case, the effect of CP should be only on electric contact amelioration. In addition, the possibility of in situ synthesis of cathode materials starting from precursors hosted into the three-dimension fibrous matrix of CP opens new and interesting prospects for this substrate-current collector.

Acknowledgements

Research funded by COFIN2002 (nanostructured alloys as anodes for Li-ion batteries). The authors thank the group of Prof. G. Cocco (University of Sassari), partner of the Project, for the mechanochemical preparation of the nanometric Cu_6Sn_5 alloy, and Dr. R. Berti (Department of Physics, University of Bologna) for the useful suggestions in SEM analysis.

References

- [1] M. Winter, J.O. Besenhard, *Electrochim. Acta* 45 (1999) 31–50.
- [2] K.D. Kepler, J.T. Vaughey, M.M. Thackeray, *Electrochem. Solid State Lett.* 2 (1999) 307–309.
- [3] D. Larcher, L.Y. Beaulieu, D.D. MacNeil, J.R. Dahn, *J. Electrochem. Soc.* 147 (2000) 1658–1662.
- [4] J. Yang, Y. Takeda, N. Imanishi, T. Ichikawa, O. Yamamoto, *J. Power Sources* 79 (1999) 220–224.
- [5] J. Wolfenstine, S. Campos, D. Foster, J. Read, W.K. Behl, *J. Power Sources* 109 (2002) 230–233.
- [6] Y. Liu, J.Y. Xie, J. Yang, *J. Power Sources* 119–121 (2003) 572–575.
- [7] W.X. Chen, J.Y. Lee, Z. Liu, *Electrochem. Commun.* 4 (2002) 260–265.
- [8] Y. Wang, J.Y. Lee, T.C. Deivaraj, *J. Electrochem. Soc.* 151 (2004) A1804–A1809.
- [9] I. Kim, G.E. Blomgren, P.N. Kumta, *Electrochem. Solid State Lett.* 7 (2004) A44–A48.
- [10] I. Isaev, G. Salitra, A. Soffer, Y.D. Aurbach, *Proceedings of the 12th International Meeting on Lithium Batteries*, Nara, Abstract 96, 2004.
- [11] Z. Chen, J. Li, V. Chevrier, L. Christensen, J.R. Dahn, *Proceedings of the 12th International Meeting on Lithium Batteries*, Nara, Abstract 4, 2004.
- [12] C. Arbizzani, M. Lazzari, M. Mastragostino, *J. Electrochem. Soc.* 152 (2005) A289–A294.
- [13] C. Arbizzani, S. Beninati, M. Lazzari, M. Mastragostino, *J. Power Sources* 141 (2005) 149–155.
- [14] J. Gong, G. Zangari, *Mater. Sci. Eng.* A344 (2003) 268–278.
- [15] L.Y. Beaulieu, D. Larcher, R.A. Dunlap, J.R. Dahn, *J. Electrochem. Soc.* 147 (2000) 3206–3212.
- [16] L.Y. Beaulieu, J.R. Dahn, *J. Electrochem. Soc.* 147 (2000) 3237–3241.
- [17] R. Moshtev, B. Johnson, *J. Power Sources* 91 (2000) 86–91.